Mean solutions for the Kuramoto-Sivashinsky equation with incoming boundary conditions

Youichi Kitahara*
Department of Earth System Science and Technology, Interdisciplinary Graduate School of Engineering Sciences, Kyushu University, Kasuga 816-8580, Japan

Makoto Okamura†
Research Institute for Applied Mechanics, Kyushu University, Kasuga 816-8580, Japan
(Received 25 December 2003; published 18 November 2004)

We consider herein the Kuramoto-Sivashinsky (KS) equation with incoming boundary conditions. Using a projection operator method, we have derived a set of closed equations for the mean quantities, called a model equation, from the KS equation. One of the characteristics of the model equation is that it does not include any empirical parameters. The adequacy of the model equation is verified by comparing solutions of the model equation with time-averaged solutions obtained from the numerical simulation of the KS equation.

DOI: 10.1103/PhysRevE.70.056210 PACS number(s): 05.45.−a, 47.52.+j, 47.27.Eq, 47.27.Qb

I. INTRODUCTION

Although the solutions of chaotic equations are not predictable, the mean or large-scale components of these equations are predictable. The ability to predict the mean quantity is important, especially in turbulent flows. In the present paper, we consider the KS equation, rather than the Navier-Stokes equation, because it is one of the simplest partial differential equations for treating chaos or turbulence.

Yakhot [1] suggested that the large-scale properties of the KS equation with random initial conditions can be modeled by a noisy Burgers equation using the dynamic renormalization group (RG) method. The dynamic RG method has also been applied to the KS equation with random forcing in the field of surface growth [2,3]. The dynamic RG method adequately predicts both the roughness exponent and the dynamic exponent which characterize the scaling laws of the interface width.

However, although it is possible to determine the ratio D/ν^3 of the noise strength squared D to the cube of the effective diffusion constant ν from the fixed points of the RG flow equation, D and ν remain unresolved. Hence it is necessary to rely on numerical simulation in order to determine the effective diffusion constant, which is an important value for obtaining information on mean quantities. Some numerical simulations have estimated the effective diffusion constant ν to be $\nu \approx 10$ for infinitely large scales with periodic boundary conditions [4,5] and with fixed boundary conditions [6].

So far, only second-order statistical quantities such as the interface width and energy spectrum have been investigated for the KS equation because the first-order statistical quantity is zero and thus unimportant for the KS equation with periodic boundary conditions. Sakaguchi [6] numerically studied the KS equation with fixed boundary conditions and estimated the effective diffusion constant from its shocklike mean solution.

In accordance with Yakhot's suggestion, we can assume that the ensemble average $\langle u \rangle$ of a solution u for the KS equation satisfies the Burgers equation

$$\frac{\partial \langle u \rangle}{\partial t} - \langle u \rangle \frac{\partial \langle u \rangle}{\partial x} - \nu \frac{\partial^2 \langle u \rangle}{\partial x^2} = 0, \tag{1.1}$$

where ν is the effective diffusion constant. The constant ν is an empirical parameter because its value cannot be determined by the dynamic RG method. The closed equation (1.1) of the mean quantity $\langle u \rangle$ is called a model equation of the KS equation. The solution of the model equation is in good agreement with the time-averaged numerical profile of the KS equation under certain fixed boundary conditions [6] if a suitable value is chosen for the undetermined parameter ν.

In the present paper, we derive another model equation for the KS equation using the projection operator method. One of the characteristics of the derived model equation is that it does not include any undetermined parameters such as ν. The procedure is similar to that reported by Sato and Okamura [8], who derived an averaged equation from a forced pendulum equation. However, the present calculation is rather complicated because, unlike the pendulum equation which is an ordinary equation, the KS equation is a partial differential equation in one-dimensional space. We examine the adequacy of the model equation by comparing its solutions with time-averaged numerical solutions of the KS equation.

II. DERIVATION OF AN AVERAGED EQUATION

We treat the KS equation

$$\frac{\partial u}{\partial t} - u \frac{\partial u}{\partial x} + \frac{\partial^2 u}{\partial x^2} + \frac{\partial^4 u}{\partial x^4} = 0, \tag{2.1}$$

with fixed boundary conditions

*Present address: Knowledge Media Laboratory, Corporate Research & Development Center, Toshiba Corporation.
†Electronic address: okamura@riam.kyushu-u.ac.jp

$$u(-\infty,t) = -U_\infty, \quad u(\infty,t) = U_\infty, \tag{2.2}$$

where U_∞ is a given constant. The fixed boundary conditions are used here instead of incoming boundary conditions (4.2) because theoretically it is difficult to treat the incoming boundary conditions at infinity. Note that both the fixed and the incoming boundary conditions for averaging give the same expressions,

$$\langle u(-\infty,t)\rangle = -U_\infty, \quad \langle u(\infty,t)\rangle = U_\infty.$$

Using the variable transform

$$y = \tanh Kx, \tag{2.3}$$

where K is a given constant, we obtain from the KS equation (2.1) and the boundary conditions (2.2)

$$\frac{\partial u}{\partial t} = c_1 u\frac{\partial u}{\partial y} + c_2\frac{\partial u}{\partial y} + c_3\frac{\partial^2 u}{\partial y^2} + c_4\frac{\partial^3 u}{\partial y^3} + c_5\frac{\partial^4 u}{\partial y^4}, \tag{2.4}$$

with boundary conditions

$$u(-1,t) = -U_\infty, \quad u(1,t) = U_\infty, \tag{2.5}$$

where

$$c_1 = K(1-y^2),$$

$$c_2 = -2K^2y(1-y^2)(8K^2 - 1 - 12K^2y^2),$$

$$c_3 = K^2(1-y^2)^2(8K^2 - 1 - 36K^2y^2),$$

$$c_4 = 12K^4y(1-y^2)^3,$$

$$c_5 = -K^4(1-y^2)^4.$$

Using an N-truncated series of Chebyshev polynomials of the first kind $T_m(y)$, we approximate $u(y,t)$ as

$$u(y,t) = \sum_{m=0}^{N} \hat{u}_m(t)T_m(y). \tag{2.6}$$

Chebyshev transformation of Eq. (2.4) and elimination of the highest terms $\hat{u}_{N-1}(t)$, $\hat{u}_N(t)$ yield $N-2$ time evolution equations,

$$\frac{d\hat{u}_m(t)}{dt} = N_m[\hat{\boldsymbol{u}}(t)] + \sum_{j=1}^{N-2} L_{mj}\hat{u}_j(t) + F_m,$$

$$m = 1,2,\ldots,N-2, \tag{2.7}$$

where $N_m[\hat{\boldsymbol{u}}(t)]$, $\Sigma_{j=1}^{N-2} L_{mj}\hat{u}_j(t)$, and F_m denote nonlinear, linear, and forcing terms, respectively. There is no forcing term in the KS equation (2.1) itself, whereas Eq. (2.7) has a forcing term which arises from the fixed boundary conditions.

We introduce a projection operator $\mathcal{P}$ as

$$\mathcal{P}f(\hat{\boldsymbol{u}}) \equiv \frac{\langle f(\hat{\boldsymbol{u}})\hat{u}_1\rangle}{\langle \hat{u}_1^2\rangle}\hat{u}_1, \tag{2.8}$$

where $f(\hat{\boldsymbol{u}})$ is an arbitrary function of $\hat{\boldsymbol{u}}$ and $\hat{u}_m \equiv \hat{u}_m(0)$. Using the projection operator [7], we can transform the nonlinear term $N_m[\hat{\boldsymbol{u}}(t)]$ into

$$\begin{aligned} N_m[\hat{\boldsymbol{u}}(t)] &= e^{\Lambda t}[\mathcal{P}N_m(\hat{\boldsymbol{u}}) + \mathcal{Q}N_m(\hat{\boldsymbol{u}})] \\ &= \Omega_m\hat{u}_1(t) - \int_0^t \Gamma_m(s)\hat{u}_1(t-s)ds + r_m(t), \end{aligned} \tag{2.9}$$

where

$$\mathcal{Q} \equiv 1 - \mathcal{P},$$

$$\Omega_m \equiv \frac{\langle N_m\hat{u}_1\rangle}{\langle \hat{u}_1^2\rangle},$$

$$\Gamma_m(t) \equiv -\frac{\langle[\Lambda r_m(t)]\hat{u}_1\rangle}{\langle \hat{u}_1^2\rangle}, \tag{2.10}$$

$$r_m(t) \equiv \exp(t\mathcal{Q}\Lambda)\mathcal{Q}N_m. \tag{2.11}$$

The first term of the right-hand side of Eq. (2.9) denotes the projected term showing coherent motion. The second term is also related to coherent motion, which is extracted from the unprojected term. The memory function $\Gamma_m(t)$ in the second term has an effect on the time dependent dissipation due to chaotic mixing, which corresponds to the eddy viscosity in turbulence. The last term $r_m(t)$ is considered to be a fluctuating force because $r_m(t)$ is related to the unprojected part $\mathcal{Q}N_m$ and its time evolution may be very complicated. A time evolution operator Λ is defined as

$$\Lambda \equiv \sum_{n=1}^{N-2}\left[N_n(\hat{\boldsymbol{u}}) + \sum_{j=1}^{N-2} L_{nj}\hat{u}_j + F_n\right]\frac{\partial}{\partial \hat{u}_n}.$$

Now we make three assumptions in order to derive an averaged equation from Eq. (2.7).

Assumption 1. No correlation for an infinite time:

$$\lim_{t\to\infty}\langle \hat{u}_m(t)\hat{u}_1\rangle = \lim_{t\to\infty}\langle \hat{u}_m(t)\rangle\langle \hat{u}_1\rangle.$$

Assumption 2. Steady state for an infinite time:

$$\lim_{t\to\infty}\frac{d}{dt}\langle \hat{u}_m(t)\hat{u}_1\rangle = 0.$$

Assumption 3. Loss of memory effect for large time:

$$\int_0^\infty |\Gamma_m(s)|ds < \infty.$$

Note that Assumption 3 gives the relation

$$\lim_{t\to\infty}\int_0^t \Gamma_m(s)\hat{u}_1(t-s)ds = \lim_{t\to\infty}\hat{u}_1(t)\int_0^\infty \Gamma_m(s)ds.$$

Using the above assumptions and Eq. (2.7), we obtain an averaged equation:

$$\Omega_m\langle\hat{u}_1(\infty)\rangle + \sum_{i=1}^{N-2} L_{mi}\langle\hat{u}_i(\infty)\rangle - \gamma_m\langle\hat{u}_1(\infty)\rangle + F_m = 0, \tag{2.12}$$

where

$$\gamma_m \equiv \int_0^\infty \Gamma_m(t)dt. \tag{2.13}$$

The averaged equation is derived under reasonable assumptions but is not a closed equation for mean quantity $\langle\hat{u}_i(\infty)\rangle$ because γ_m includes higher-order moments and depends on the time history.

We now show that the memory function $\Gamma_m(t)$ can be evaluated numerically as follows [9,10]. Referring to Appendix A, we can rewrite the memory function $\Gamma_m(t)$, Eq. (2.10), as

$$\begin{aligned}\Gamma_m(t_0) = \psi_m(t_0) &- \int_0^{t_0} dt_1 \psi_m(t_1)\phi(t_0-t_1) \\ &+ \int_0^{t_0} dt_1 \int_0^{t_1} dt_2 \psi_m(t_2)\phi(t_1-t_2)\phi(t_0-t_1) \\ &- \cdots + (-1)^n \int_0^{t_0} dt_1 \cdots \int_0^{t_{n-1}} dt_n \psi_m(t_n) \\ &\times \underbrace{\phi(t_{n-1}-t_n)\cdots\phi(t_0-t_1)}_{n} + \cdots,\end{aligned} \tag{2.14}$$

where

$$\psi_m(t) = -\phi_m^N(t) + \Omega_m\phi(t), \tag{2.15}$$

$$\phi_m^N(t) = \frac{1}{\langle\hat{u}_1^2\rangle}\left\langle \frac{dN_m[\hat{\boldsymbol{u}}(t)]}{dt}\hat{u}_1 \right\rangle, \tag{2.16}$$

$$\phi(t) = \frac{1}{\langle\hat{u}_1^2\rangle}\left\langle \frac{d\hat{u}_1(t)}{dt}\hat{u}_1 \right\rangle. \tag{2.17}$$

We can evaluate the values of the right-hand side of Eqs. (2.16) and (2.17) through numerical simulation. Laplace transform of Eq. (2.14) and formula (B2) yield

$$\overline{\Gamma}_m(z) = -\frac{\overline{\phi}_m^N(z) - \Omega_m\overline{\phi}(z)}{1+\overline{\phi}(z)},$$

where $\overline{\Gamma}_m(z)$, $\overline{\phi}_m^N(z)$, and $\overline{\phi}(z)$ are Laplace transforms of $\Gamma_m(t)$, $\phi_m^N(t)$, and $\phi(t)$, respectively. The memory function $\Gamma_m(t)$ can thus be evaluated.

III. MODEL EQUATION

It is possible to evaluate γ_m in Eq. (2.12) exactly by using Eq. (2.14). However, the result is trivial and provides no useful information about mean quantity $\langle\hat{u}_m\rangle$ as shown in Appendix B. Instead we can approximately evaluate γ_m, which is a function of $\Gamma_m(t)$, by using $\Gamma_m \equiv \Gamma_m(0)$ and $\dot{\Gamma}_m \equiv \dot{\Gamma}_m(0)$. Here, we make an assumption about the memory function form.

Assumption 4. Form of memory function:

$$\Gamma_m(t) = \Gamma_m \exp(-\alpha_m t), \quad \alpha_m > 0. \tag{3.1}$$

The first-order Taylor expansion of Eq. (3.1) around $t=0$ shows

$$\dot{\Gamma}_m = -\Gamma_m\alpha_m. \tag{3.2}$$

From Eqs. (3.1), (3.2), and (2.13) we obtain

$$\gamma_m = -\frac{\Gamma_m^2}{\dot{\Gamma}_m},$$

where

$$\Gamma_m = \psi_m(0), \tag{3.3}$$

$$\dot{\Gamma}_m = \dot{\psi}_m(0) - \psi_m(0)\phi(0). \tag{3.4}$$

We have other expressions for Γ_m and $\dot{\Gamma}_m$ such as

$$\Gamma_m = -\frac{\langle[\Lambda\mathcal{Q}N_m]\hat{u}_1\rangle}{\langle\hat{u}_1^2\rangle}, \tag{3.5}$$

$$\dot{\Gamma}_m = -\frac{\langle[\Lambda(\mathcal{Q}\Lambda)\mathcal{Q}N_m]\hat{u}_1\rangle}{\langle\hat{u}_1^2\rangle}, \tag{3.6}$$

which appeared in the paper by Sato and Okamura [8]. The present expressions (3.3) and (3.4) are simpler than Eqs. (3.5) and (3.6) because operators such as Λ and $\mathcal{Q}$ are not included. Note that we make no assumptions for the Markov process such as $\Gamma_m(t) \propto \delta(t)$.

Here, we make further assumptions.

Assumption 5. Symmetry of mean value:

$$\langle\hat{u}_m(\infty)\rangle = 0, \quad \text{if } m \text{ is even}.$$

The KS equation has an antisymmetry solution under the antisymmetry initial and boundary conditions because the KS equation is invariant under transformations $x\to -x$ and $u\to -u$. However, a numerical solution breaks antisymmetry because of its chaotic characteristics and numerical errors, while its mean solution is expected to have antisymmetry.

Assumption 6. Zero variance:

$$\langle\hat{u}_m^n\rangle = \langle\hat{u}_m\rangle^n. \tag{3.7}$$

Numerical results show that the representative scale of the mean profile is much larger than that of chaotic or fluctuating motion [6] and hence Eq. (3.7) is a good approximation for smaller m, while Eq. (3.7) is likely to be invalid for larger m because

$$\langle \hat{u}_m^n \rangle \gg \langle \hat{u}_m \rangle^n \approx 0.$$

However, the invalidity of Eq. (3.7) for larger m has little influence on the derivation of a model equation because $\langle \hat{u}_m \rangle$ rapidly approaches zero for larger m:

$$\langle \hat{u}_m \rangle = O(\epsilon^m), \quad \epsilon \ll 1. \tag{3.8}$$

Assumption 6 is therefore a good approximation due to separation between the scale of mean profile and that of chaotic motion. This assumption may be the most disputable among those made in the present study.

Assumption 7. Initial value on the attractor:

$$\langle \hat{u}_m \rangle = \langle \hat{u}_m(\infty) \rangle. \tag{3.9}$$

Condition (3.9) does not generally mean an initial value on the attractor. However, the variance for the main components is small and thus

$$\hat{u}_m \approx \langle \hat{u}_m \rangle, \quad \hat{u}_m(\infty) \approx \langle \hat{u}_m(\infty) \rangle,$$

for small m, which is consistent with Assumption 7. For large m, Eq. (3.9) is also satisfied approximately because of

$$\langle \hat{u}_m \rangle \approx 0, \quad \langle \hat{u}_m(\infty) \rangle \approx 0,$$

although

$$\hat{u}_m \neq \langle \hat{u}_m \rangle.$$

From Eqs. (3.7), (3.9), and (2.12) we obtain a model equation

$$\Omega_m \langle \hat{u}_1 \rangle + \sum_{i=1}^{N-2} L_{mi} \langle \hat{u}_i \rangle - \gamma_m \langle \hat{u}_1 \rangle + F_m = 0,$$

$$m = 1,2, \ldots, N-2, \tag{3.10}$$

which is a closed nonlinear algebraic equation of $\langle \hat{u}_m \rangle$. The highest order term $\langle \hat{u}_N \rangle$ is determined from Eq. (2.5).

IV. COMPARISON OF MODEL SOLUTIONS AND NUMERICAL RESULTS

In this section, we compare solutions of the model equation (3.10) and numerical solutions of the KS equation (2.1) with incoming boundary conditions (4.2).

A. Numerical conditions

We have used a finite difference method for the spatial derivative and the fourth-order Runge-Kutta method for time evolution. The spatial difference Δx and the time step Δt are chosen to be $\Delta x = 0.33$ and $\Delta t = 0.0002$, respectively. The system size L is $L = 400$. The antisymmetry initial condition is chosen to be

$$u(x,0) = \begin{cases} U_{\mathrm{nu}} + 0.1 \sin(x/\sqrt{2}), & \text{for } x \geqslant 0, \\ -U_{\mathrm{nu}} + 0.1 \sin(x/\sqrt{2}), & \text{for } x < 0, \end{cases} \tag{4.1}$$

where $1/\sqrt{2}$ is the wave number of the most unstable mode and U_{nu} is a given parameter. The incoming boundary conditions at $x = \pm L/2$ are

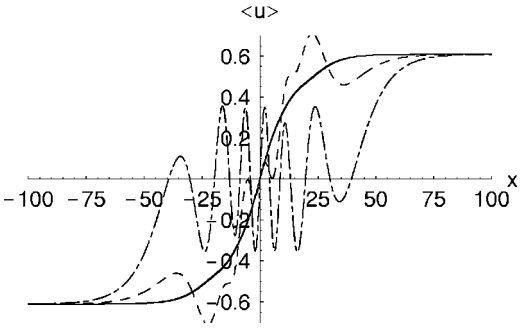

FIG. 1. Three types of solutions of the model equation (3.10) for $U_\infty = 0.61$, $K = 0.05$, and $N = 13$: —·—, type I; – – – –, type II; —, type III.

$$u(L/2,t) = u_p^+(0,t), \quad u(-L/2,t) = u_p^-(0,t), \tag{4.2}$$

where $u_p^+(x,t)$ and $u_p^-(x,t)$ are solutions of the KS equation (2.1) with a periodic boundary condition under

$$\frac{1}{L} \int_{-L/2}^{L/2} u_p^+(x,t) dx = U_{\mathrm{nu}},$$

and

$$\frac{1}{L} \int_{-L/2}^{L/2} u_p^-(x,t) dx = -U_{\mathrm{nu}},$$

respectively. Since profiles at $x = -L/2$ and $x = L/2$ travel to the right and to the left, respectively, we have called Eq. (4.2) the incoming boundary condition. It is easy to show that u_p^+ travels to the left by transformations $U = u_p^+ - U_{\mathrm{nu}}$, $X = x + U_{\mathrm{nu}} t$, and $T = t$. Note that the boundary conditions (4.2) differ from those by Sakaguchi [6].

The average for numerical data is obtained by time averaging defined as

$$\overline{u}(x) = \frac{1}{T - T_0} \int_{T_0}^{T} u(x,t) dt, \tag{4.3}$$

where T_0 is selected in order to discard data far from the attractor and we set $T_0 = 1000$. The ensemble average for $t > T_0$ is independent of time as a result of statistical stationarity, and hence we assume that the ensemble average agrees with the time average due to ergodicity. We have made a correction

$$u(x,t) - \frac{1}{L} \int_{-L/2}^{L/2} u(x,t) dx \to u(x,t)$$

at every time step in order to maintain antisymmetry for the mean profile.

B. Convergence of model solution

We solve the nonlinear algebraic equation (3.10) for $\langle \hat{u}_m \rangle$ using Newton's method. Since the equation is extremely complicated, we have omitted the terms of order higher than $O(K^7)$ and $O(\epsilon^N)$ where K and ϵ are assumed to be small parameters. K is concerned with the variable transform (2.3)

TABLE I. Values of κ and its number for three types of solutions.

Type of solutions	Value of κ	Number of κ
Type I	$\kappa=0.001$	1
Type II	$\kappa=0.006$	1
	$\kappa=0.024$, 0.062,	
	$0.031\leqslant\kappa\leqslant0.043$	
Type III	$0.053\leqslant\kappa\leqslant0.054$	24
	$0.057\leqslant\kappa\leqslant0.06$	
	$0.068\leqslant\kappa\leqslant0.07$	
Nonconvergence	others	44

and we have chosen $0.015\leqslant K\leqslant0.07\ll1$ in this paper. ϵ is the amplitude of $\langle\hat{u}_1\rangle$ and $\langle\hat{u}_n\rangle=O(\epsilon^n)$ is assumed. N is the truncation order of the Chebyshev polynomials in Eq. (2.6).

First, we consider the dependence of the solution $\langle\hat{u}_m\rangle$ on an initial value $\langle\hat{u}_m\rangle_{\rm ini}$ of the iteration for given values of K and U_∞. Solving the nonlinear equation (3.10) with various initial values of the iteration,

$$\langle u(x)\rangle_{\rm ini}=U_\infty\tanh\,\kappa x,$$

where $\kappa=0.001\times i$, $i=1,2,\ldots,70$, we obtain three types of solutions depending on the initial values for $U_\infty=0.61$, $K=0.06$, and $N=13$. Figure 1 shows the three types of solutions denoted by dot-dashed, broken, and solid curves which are referred to as types I, II, and III, respectively. Table I shows the convergence of solutions for various values of κ. A convergent solution can be found for each of 26 among 71 values of κ, and 24 among the 26 convergent solutions are type III. It is therefore reasonable to choose type III as the solution of the model equation in this case.

Second, we consider the dependence of the solution $\langle\hat{u}_m\rangle$ on the truncation order N for $K=0.06$ and $U_\infty=0.61$. Figure 2 shows the solutions for $N=11$ (dot-dashed curve), $N=13$ (broken curve), and $N=15$ (solid curve). Since the solutions for $N=13$ and $N=15$ are very close, the number of $N=13$ is enough to obtain the convergent solution as regards N in this case. Note that a necessary number of N to obtain the convergent solution depends on U_∞.

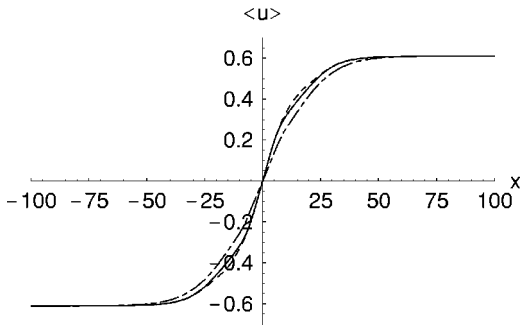

FIG. 2. Solutions of the model equation (3.10) for three truncation orders: —·—, $N=11$; – – – –, $N=13$; —, $N=15$.

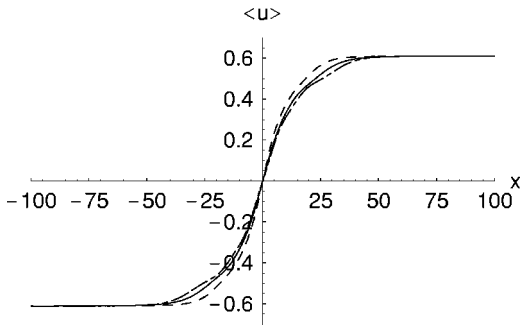

FIG. 3. Solutions of the model equation (3.10) for three parameters: —, $K=0.05$; —·—, $K=0.06$; – – – –, $K=0.07$.

Finally, we consider the dependence of the solution $\langle\hat{u}_m\rangle$ on the variable transform parameter K in Eq. (2.3) for $N=13$, $U_\infty=0.61$, and $\kappa=0.06$. Calculating five cases of $K=0.01\times i$, $i=4,5,\ldots,8$, we have found a convergent solution for each of the three cases $K=0.05$, 0.06, and 0.07. Figure 3 shows the solutions for $K=0.05$, 0.06, 0.07. Note that the solutions for $K=0.04$ and $K=0.08$ may also converge for other values of κ. Model solutions in Fig. 3 depend weakly on the parameter K because we have omitted the terms of order higher than $O(K^{N_1})$, $N_1=7$ and $O(\epsilon^N)$, $N=13$. Appropriate selection of K yields the convergent solution and the most appropriate selection does the solution for the smallest truncation number N. Furthermore, we could obtain the same solution for various values of K only if we choose large enough values of N and N_1, because the parameter K is related to the variable transform (2.3). We can hence expect that the model solutions are independent of the parameter K for $N_1\to\infty$ and $N\to\infty$.

C. Results

We compare numerical solutions of the KS equation for three cases of $U_{\rm nu}=0.3,0.5,0.7$ with solutions of the model equation (3.10) for the values of U_∞ corresponding to $U_{\rm nu}$. Each value of U_∞ is chosen in order to closely fit a numerical solution to a model solution.

Figure 4 shows the time-averaged numerical solution (thick curve) for $U_{\rm nu}=0.3$ and the model solution (thin curve) for $N=15$, $K=0.035$, $\kappa=0.031$, and $U_\infty=0.39$. The final time in Eq. (4.3) is $T=200\,000$. The time-averaged solution

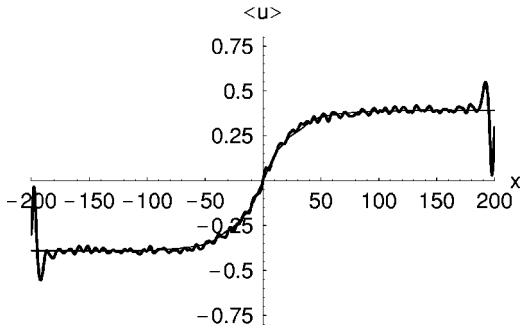

FIG. 4. Model solution (thin curves) of Eq. (3.10) for $U_\infty=0.39$ and numerical solution (thick curves) for $U_{\rm nu}=0.3$.

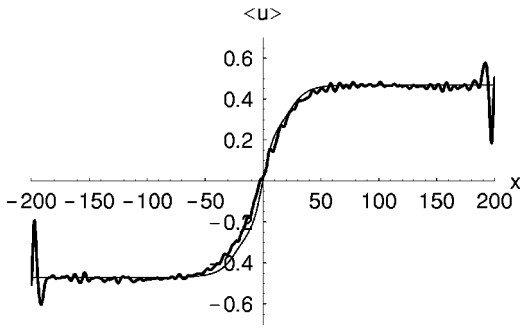

FIG. 5. Model solution (thin curves) of Eq. (3.10) for $U_\infty = 0.47$ and numerical solution (thick curves) for $U_{\mathrm{nu}} = 0.5$.

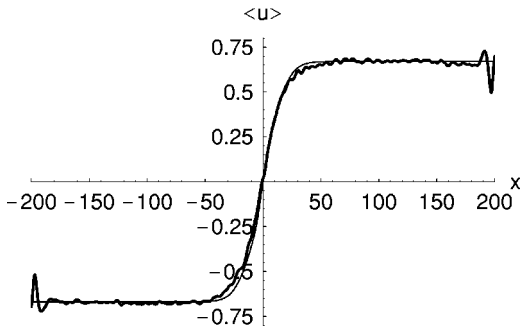

FIG. 6. Model solution (thin curves) of Eq. (3.10) for $U_\infty = 0.67$ and numerical solution (thick curves) for $U_{\mathrm{nu}} = 0.7$.

shows a small wavy disturbance corresponding to the chaotic pattern and the disturbance is expected to disappear for larger final times T. Its profile near the boundaries $x = \pm L/2$ deviates largely from the model solution due to a mismatch between Eqs. (4.1) and (4.2) at the boundaries and finiteness of the system size L, which is referred to as boundary contamination. The boundary value U_∞ differs from U_{nu} as a result of boundary contamination.

Figure 5 shows the time-averaged numerical solution (thick curve) for $U_{\mathrm{nu}} = 0.5$ and the model solution (thin curve) for $N = 15$, $K = 0.05$, $\kappa = 0.038$, and $U_\infty = 0.47$. The final time in Eq. (4.3) is $T = 200\,000$.

Figure 6 shows the time-averaged numerical solution (thick curve) for $U_{\mathrm{nu}} = 0.7$ and the model solution (thin curve) for $N = 15$, $K = 0.065$, $\kappa = 0.06$, and $U_\infty = 0.67$. The final time in Eq. (4.3) is $T = 200\,000$. Note that the boundary contamination in Fig. 6 is the smallest among our results.

Agreement of the numerical results with the model solutions is fairly good. Note that there is a slight ambiguity for the model solutions due to the dependence of the solutions on K because of the omission of higher-order terms, as shown in Fig. 3.

V. CONCLUDING REMARKS AND DISCUSSION

We derived a closed equation for mean value $\langle \hat{u}_m \rangle$ from the KS equation using a projection operator. Good agreement between solutions of the model equation and numerical solutions shows that the projection operator method is useful for the derivation of an average equation from the KS equation.

We next comment on the projection operator $\mathcal{P}$ defined in Eq. (2.8). The operator projects onto only $\hat{u}_1$ and thus

$$\mathcal{P}\hat{u}_1 = \hat{u}_1,$$

and

$$\mathcal{P}\hat{u}_m \neq \hat{u}_m, \quad m \neq 1.$$

Another candidate for a projection operator is [7]

$$\mathcal{P}_F f(\hat{\boldsymbol{u}}) \equiv \sum_{n=1}^{N-2} \sum_{m=1}^{N-2} \langle f(\hat{\boldsymbol{u}}) \hat{u}_n \rangle [\langle \hat{\boldsymbol{u}} \hat{\boldsymbol{u}}^\dagger \rangle^{-1}]_{nm} \hat{u}_m,$$

where $\dagger$ denotes the Hermitian conjugate and $f(\hat{\boldsymbol{u}})$ is an arbitrary function of $\hat{\boldsymbol{u}}$. The operator $\mathcal{P}_F$ has a preferable characteristic,

$$\mathcal{P}_F \hat{u}_m = \hat{u}_m,$$

while the derivation of a model equation is much more complicated if we use $\mathcal{P}_F$ instead of $\mathcal{P}$. The difference between $\mathcal{P}_F$ and $\mathcal{P}$ is not so large because $\hat{u}_1$ is the main component due to Eq. (3.8), and hence we can expect that the results obtained by using $\mathcal{P}_F$ agree well with those by $\mathcal{P}$.

The KS equation has two different spatial scales which correspond to chaotic motion and the representative change of mean values. The scales are separate from each other, which means that the ratio of the scale of mean values to that of chaotic motion is very large. This is one of the main reasons why the present results, obtained by the projection operator method, are satisfactory. It should be interesting to apply this method to a problem for which the representative scale of chaotic motion is similar to that of the mean values, such as the problem of the energy spectrum of the KS equation with a periodic boundary condition.

ACKNOWLEDGMENT

The authors would like to express their thanks to Dr. K. Ueno of Kyushu University for his valuable discussions on the dynamic RG method.

APPENDIX A: EXACT EVALUATION OF MEMORY FUNCTION

Using an identity

$$e^{t\mathcal{Q}\Lambda} = e^{t\Lambda} - \int_0^t dt_1 e^{(t-t_1)\Lambda} \mathcal{P}\Lambda e^{t_1 \mathcal{Q}\Lambda}, \tag{A1}$$

we delete $\mathcal{Q}$ in the left-hand side of Eq. (A1) iteratively and then obtain

$$e^{t\mathcal{Q}\Lambda} = e^{t\Lambda} - \int_0^t dt_1 e^{(t-t_1)\Lambda}\mathcal{P}\Lambda e^{t_1\Lambda} + \int_0^t dt_1 \int_0^{t_1} dt_2 e^{(t-t_1)\Lambda}\mathcal{P}\Lambda e^{(t_1-t_2)\Lambda}\mathcal{P}\Lambda e^{t_2\Lambda}$$
$$- \int_0^t dt_1 \int_0^{t_1} dt_2 \int_0^{t_2} dt_3 e^{(t-t_1)\Lambda}\mathcal{P}\Lambda e^{(t_1-t_2)\Lambda}\mathcal{P}\Lambda e^{(t_2-t_3)\Lambda}\mathcal{P}\Lambda e^{t_3\Lambda} + \cdots$$
$$+ (-1)^n \int_0^t dt_1 \int_0^{t_1} dt_2 \cdots \int_0^{t_{n-1}} dt_n e^{(t-t_1)\Lambda}\mathcal{P}\Lambda e^{(t_1-t_2)\Lambda}\mathcal{P}\Lambda \cdots e^{(t_{n-1}-t_n)\Lambda}\mathcal{P}\Lambda e^{t_n\Lambda} + \cdots . \tag{A2}$$

From Eqs. (A2), (2.11), and (2.10) we obtain

$$\Gamma_m(t) = -\frac{\langle[\Lambda e^{t\Lambda}\mathcal{Q}N_m]\hat{u}_1\rangle}{\langle\hat{u}_1^2\rangle} + \int_0^t dt_1 \frac{\langle[\Lambda e^{t_1\Lambda}\mathcal{Q}N_m]\hat{u}_1\rangle}{\langle\hat{u}_1^2\rangle}\frac{\langle[\Lambda e^{(t-t_1)\Lambda}\hat{u}_1]\hat{u}_1\rangle}{\langle\hat{u}_1^2\rangle}$$
$$- \int_0^t dt_1 \int_0^{t_1} dt_2 \frac{\langle[\Lambda e^{t_2\Lambda}\mathcal{Q}N_m]\hat{u}_1\rangle}{\langle\hat{u}_1^2\rangle}\frac{\langle[\Lambda e^{(t_1-t_2)\Lambda}\hat{u}_1]\hat{u}_1\rangle}{\langle\hat{u}_1^2\rangle}\frac{\langle[\Lambda e^{(t-t_1)\Lambda}\hat{u}_1]\hat{u}_1\rangle}{\langle\hat{u}_1^2\rangle}$$
$$- (-1)^n \int_0^t dt_1 \int_0^{t_1} dt_2 \cdots \int_0^{t_{n-1}} dt_n \frac{\langle[\Lambda e^{t_n\Lambda}\mathcal{Q}N_m]\hat{u}_1\rangle}{\langle\hat{u}_1^2\rangle}\frac{\langle[\Lambda e^{(t_{n-1}-t_n)\Lambda}\hat{u}_1]\hat{u}_1\rangle}{\langle\hat{u}_1^2\rangle}\cdots\frac{\langle[\Lambda e^{(t-t_1)\Lambda}\hat{u}_1]\hat{u}_1\rangle}{\langle\hat{u}_1^2\rangle} + \cdots . \tag{A3}$$

Using the relation

$$\frac{\langle[\Lambda e^{t\Lambda}\mathcal{Q}N_m]\hat{u}_1\rangle}{\langle\hat{u}_1^2\rangle} = \frac{\langle[\Lambda e^{t\Lambda}N_m]\hat{u}_1\rangle}{\langle\hat{u}_1^2\rangle} - \frac{\langle[\Lambda e^{t\Lambda}\hat{u}_1]\hat{u}_1\rangle}{\langle\hat{u}_1^2\rangle}\frac{\langle N_m\hat{u}_1\rangle}{\langle\hat{u}_1^2\rangle}$$
$$= \psi_m(t),$$

we can derive Eq. (2.14) from Eq. (A3).

APPENDIX B: INTEGRAL OF MEMORY FUNCTION

Integrating Eq. (2.14) we obtain

$$\int_0^\infty \Gamma_m(t)dt = \sum_{n=0}^\infty (-1)^n \int_0^\infty \psi_m(t)dt\left[\int_0^\infty \phi(t)dt\right]^n$$
$$= \frac{\int_0^\infty \psi_m(t)dt}{1+\int_0^\infty \phi(t)dt}, \tag{B1}$$

where we have used the formula

$$\int_0^\infty dt_0 \int_0^{t_0} dt_1 \int_0^{t_1} dt_2 \cdots \int_0^{t_{n-1}} dt_n\, f(t_n) \times g(t_{n-1}-t_n)\cdots g(t_1-t_2)g(t_0-t_1)$$
$$= \int_0^\infty f(t)dt\left[\int_0^\infty g(t)dt\right]^n. \tag{B2}$$

Integrals of Eqs. (2.16) and (2.17) yield

$$\int_0^\infty \phi_m^N(t)dt = \frac{\langle N_m[\hat{\boldsymbol{u}}(\infty)]\rangle\langle\hat{u}_1\rangle - \langle N_m(\hat{\boldsymbol{u}})\hat{u}_1\rangle}{\langle\hat{u}_1^2\rangle}, \tag{B3}$$

and

$$\int_0^\infty \phi(t)dt = \frac{\langle\hat{u}_1(\infty)\rangle\langle\hat{u}_1\rangle - \langle\hat{u}_1^2\rangle}{\langle\hat{u}_1^2\rangle}, \tag{B4}$$

respectively. We obtain a strict relation

$$\int_0^\infty \Gamma_m(t)dt = \Omega_m - \frac{\langle N_m[\hat{\boldsymbol{u}}(\infty)]\rangle}{\langle\hat{u}_1(\infty)\rangle}, \tag{B5}$$

from Eqs. (B1), (B3), (B4), and (2.15). Substituting Eq. (B5) into Eq. (2.12) we obtain

$$\sum_{j=1}^{N-2} L_{mj}\langle\hat{u}_j(\infty)\rangle + \langle N_m[\hat{\boldsymbol{u}}(\infty)]\rangle + F_m = 0, \tag{B6}$$

which is the same relation obtained from Eq. (2.7) after $t \to \infty$ and ensemble averaging, and Eq. (B6) therefore gives no useful information about mean quantity, although it is an exact relation.

[1] V. Yakhot, Phys. Rev. A **24**, 642 (1981).
[2] M. Kardar, G. Parisi, and Y. C. Zhang, Phys. Rev. Lett. **56**, 889 (1986).
[3] R. Cuerno and K. B. Lauritsen, Phys. Rev. E **52**, 4853 (1995).
[4] S. Zaleski, Physica D **34**, 427 (1989).
[5] K. Sneppen, J. Krug, M. H. Jensen, C. Jayaprakash, and T. Bohr, Phys. Rev. A **46**, R7351 (1992).
[6] H. Sakaguchi, Phys. Rev. E **62**, 8817 (2000).
[7] H. Mori and H. Fujisaka, Phys. Rev. E **63**, 026302 (2001).
[8] K. Sato and M. Okamura, Prog. Theor. Phys. **108**, 1 (2002).
[9] J. Okada, I. Sawada, and Y. Kuroda, J. Phys. Soc. Jpn. **64**, 4092 (1995).
[10] H. Mori, S. Kuroki, H. Tominaga, R. Ishizaki, and N. Mori, Prog. Theor. Phys. **109**, 333 (2003).